

1 **Convergence in amino acid outsourcing between animals and predatory bacteria**

2 Niko Kasalo¹, Mirjana Domazet-Lošo² and Tomislav Domazet-Lošo^{1,3,*}

3
4 ¹Laboratory of Evolutionary Genetics, Division of Molecular Biology, Ruđer Bošković
5 Institute, Bijenička cesta 54, HR-10000 Zagreb, Croatia

6 ²Department of Applied Computing, Faculty of Electrical Engineering and Computing,
7 University of Zagreb, Unska 3, HR-10000 Zagreb, Croatia

8 ³School of Medicine, Catholic University of Croatia

9 *Correspondence: T.D.-L. tdomazet@irb.hr

10 11 **Abstract**

12 All animals have outsourced about half of the 20 proteinogenic amino acids (AAs). We recently
13 demonstrated that the loss of biosynthetic pathways for these outsourced AAs is driven by
14 energy-saving selection. Paradoxically, these metabolic simplifications enabled animals to use
15 costly AAs more frequently in their proteomes, allowing them to explore sequence space more
16 freely. Based on these findings, we proposed that environmental AA availability and cellular
17 respiration mode are the two primary factors determining the evolution of AA auxotrophies in
18 animals. Remarkably, our recent analysis showed that bacterial AA auxotrophies are also
19 governed by energy-related selection, thereby roughly converging with animals. However,
20 bacterial AA auxotrophies are highly heterogeneous and scattered across the bacterial
21 phylogeny, making direct ecological and physiological comparisons with the animal AA
22 outsourcing model challenging. To better test the universality of our model, we focused on
23 Bdellovibrionota and Myxococcota—two closely related bacterial phyla that, through aerobic
24 respiration and a predatory lifestyle, best parallel animals. Here, we show that Bdellovibrionota,
25 driven by energy-related selection, outsourced a highly similar set of AAs to those in animals.
26 This sharply contrasts with Myxococcota, which exhibit far fewer AA auxotrophies and rarely
27 show signatures of energy-driven selection. These differences are also reflected in
28 Bdellovibrionota proteomes, which are substantially more expensive than those of
29 Myxococcota. Finally, we found evidence that the expression of costly proteins plays a crucial
30 role in the predatory phase of the Bdellovibrio life cycle. Together, our findings suggest that

31 Bdellovibrionota, through their obligate predatory lifestyle, exhibit the closest analogy to the
32 AA auxotrophy phenotype observed in animals. In contrast, facultative predation, as seen in
33 Myxococcota, appears to substantially limit the evolution of AA auxotrophies. These cross-
34 domain convergences strongly support the general validity of our AA outsourcing model.

35 **Keywords:** bacteria; predation; amino acids; animals; auxotrophy; energetics; selection;
36 evolution

37

38 **Introduction**

39 The biosynthesis of amino acids (AAs) is a fundamental biochemical process essential for
40 sustaining all life on Earth. However, despite the universal metabolic demand for all 20
41 proteinogenic AAs, some organisms have lost the ability to synthesize certain AAs
42 endogenously. The most well-known example is animals [1–3], which have lost the capacity to
43 produce approximately half of the complete AA set. A similar pattern of auxotrophies has
44 independently emerged in other eukaryotic groups, such as certain amoebae and euglenozoans
45 [1,2]. While most bacteria remain fully prototrophic [4], many bacterial lineages display
46 varying degrees of AA auxotrophy [4–6].

47 It has long been speculated that the ability to acquire AAs from the environment influences the
48 evolution of AA auxotrophies [2]. For instance, experiments have shown that bacteria
49 auxotrophic for an externally supplemented AA can gain a selective advantage over fully
50 prototrophic counterparts [7]. However, a robust theoretical framework for this phenomenon
51 remained elusive. In our previous work, we addressed this gap by proposing a model that
52 explains the evolution of AA outsourcing through several key factors: an AA is more likely to
53 be lost if (i) its biosynthesis is highly energy-demanding, (ii) it has a low pleiotropic effect, (iii)
54 it is abundantly available in the environment, and (iv) the organism relies on efficient aerobic
55 respiration for energy production [1].

56 Most importantly, we demonstrated that there is a constant selective pressure to outsource the
57 synthesis of energetically costly AAs to the environment. Surprisingly, this leads to an
58 increased usage of these expensive AAs in proteomes, allowing animal proteins to explore
59 sequence space more freely [1,8]. To determine whether these global patterns are also valid in
60 bacteria, we investigated AA auxotrophies across bacterial phylogeny and found that energy-
61 related selection also plays an important role in shaping AA outsourcing in bacteria [5].

62 However, bacteria exhibit far greater metabolic and ecological diversity than animals [4,9,10],
63 which necessitates testing our AA outsourcing model in specific bacterial groups whose
64 lifestyles more closely parallel those of animals.

65 One such group is the phylum Bdellovibrionota, which includes several aerobic or
66 microaerophilic species with an obligate predatory lifestyle [11–13]. Within this phylum,
67 predation occurs via two distinct strategies: epibiotic predation, where the bacterium attaches
68 to the prey cell and leeches nutrients from its surface, and endobiotic predation, where the
69 bacterium enters the prey cell and forms a bdelloplast, within which it feeds, grows, and divides
70 [11–13]. The life cycle of Bdellovibrionota consists of two transcriptionally distinct phases: the
71 attack phase, during which the bacterium seeks and attaches to prey, and the feeding phase,
72 characterized by growth and replication [12,14].

73 Another bacterial group exhibiting animal-like behaviors is the phylum Myxococcota, a close
74 relative of Bdellovibrionota [15,16]. Myxococcota are aerobes known for their complex
75 multicellular behaviors, including social movement in coordinated "wolf packs," fruiting body
76 formation, and predation [17]. However, unlike Bdellovibrionota, Myxococcota are not
77 obligate predators—they can scavenge nutrients from dead organic matter and survive periods
78 of starvation through sporulation [18–20].

79 The predatory lifestyle evolved independently in Bdellovibrionota and Myxococcota [16],
80 leading to vastly different phenotypic outcomes [11–13,18–20]. Thus, these two bacterial
81 groups provide an ideal system to test the predictive power of our AA outsourcing model, as
82 they allow us to directly link the evolution of AA auxotrophies in bacteria to distinct ecological
83 and physiological traits [1,5,8].

84 Here, we demonstrate that Bdellovibrionota evolved a remarkably animal-like set of AA
85 auxotrophies, accompanied by an increase in relative proteome costs. Our findings indicate that
86 energy-related selection played a key role in shaping these auxotrophies and that the attack and
87 feeding phases of their life cycle exhibit distinct energy dynamics at the transcriptomic level.
88 Surprisingly, this pattern does not hold for Myxococcota, which show fewer auxotrophies and
89 lower proteome costs, suggesting a fundamental difference in how different reliance on a
90 predatory lifestyle shapes metabolic evolution across these two groups.

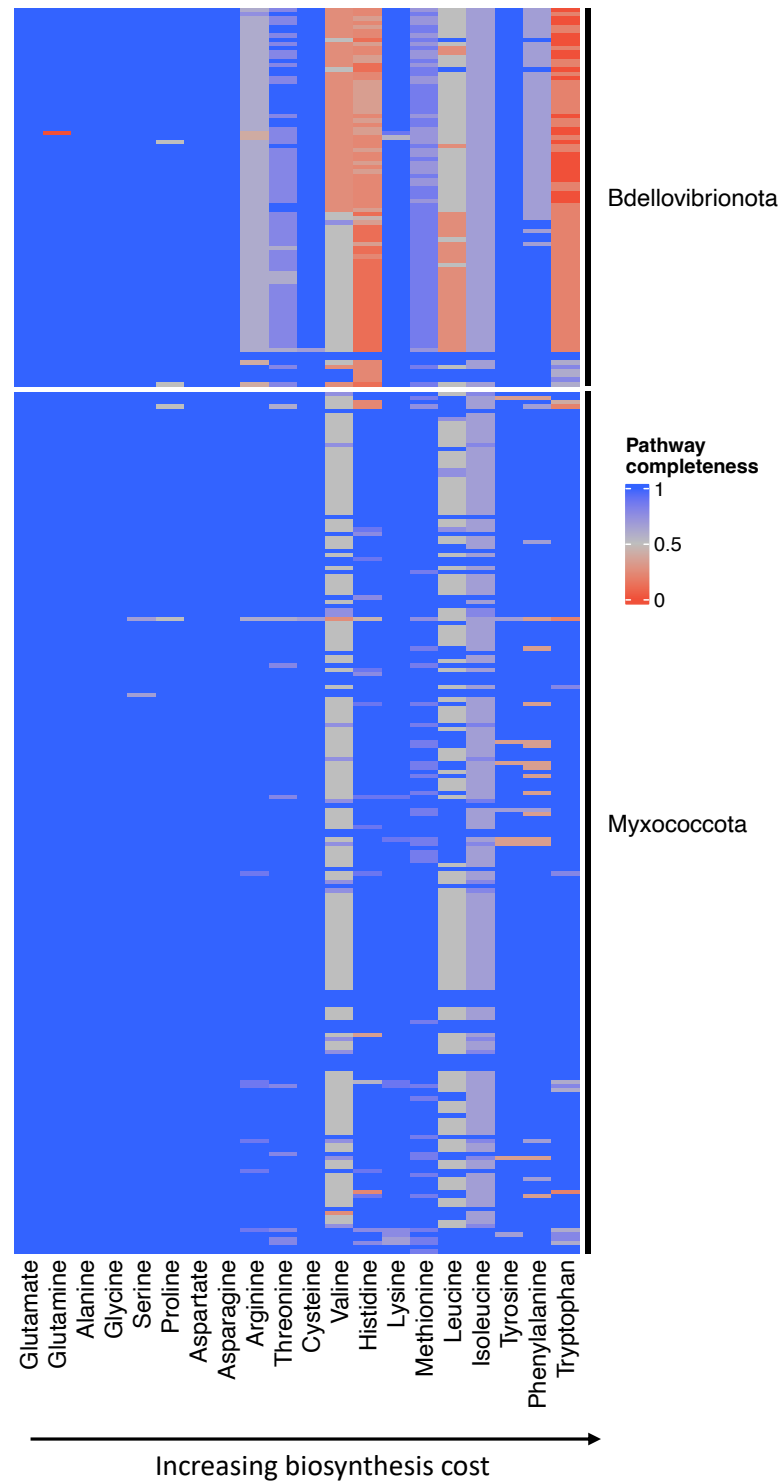
91

92

93 Results

94 We suspected that the animal-like ecophysiology of Bdellovibrionota and Myxococcota
95 imposes energy-related selection on their AA metabolism, leading to reductions in AA
96 biosynthetic pathways similar to those observed in animals. To test this hypothesis, we first
97 estimated the completeness of AA biosynthesis pathways in 89 Bdellovibrionota and 203
98 Myxococcota high-quality proteomes, which we retrieved from NCBI (Table S1). To assess
99 AA biosynthesis pathway completeness, which represents the likelihood of a given pathway
100 being present, we used the MMseqs2 clustering approach [5,21]. Heatmap representations
101 clearly revealed significantly lower AA completeness scores in Bdellovibrionota compared to
102 Myxococcota (Figure 1, File S1).

103 Most Bdellovibrionota showed reductions in pathway completeness scores for nine amino acids
104 (AAs) that fall on the expensive end of the biosynthesis cost distribution (Figure 1, File S1).
105 This set of AAs with low completeness scores largely overlaps with those that are auxotrophic
106 in animals [1], with one notable exception—lysine, which appears to be prototrophic in
107 Bdellovibrionota (Figure 1, File S1). In contrast, the pattern of AA biosynthesis pathway
108 reduction in Myxococcota is markedly different. Most Myxococcota remain prototrophic for
109 the majority of AAs, with only valine, leucine, and isoleucine biosynthesis pathways
110 consistently exhibiting reductions (Figure 1, File S1). An exception to this trend is observed in
111 two Myxococcota species—*Vulgatibacter incomptus* and *Pajaroellobacter abortibovis*—
112 which display a substantial number of AA auxotrophies (Figure S1). Taken together, these
113 findings suggest that while some reductions of expensive AA occur in Myxococcota, some
114 ecological factors likely prevent them from outsourcing most of their costly AA biosynthesis
115 pathways.

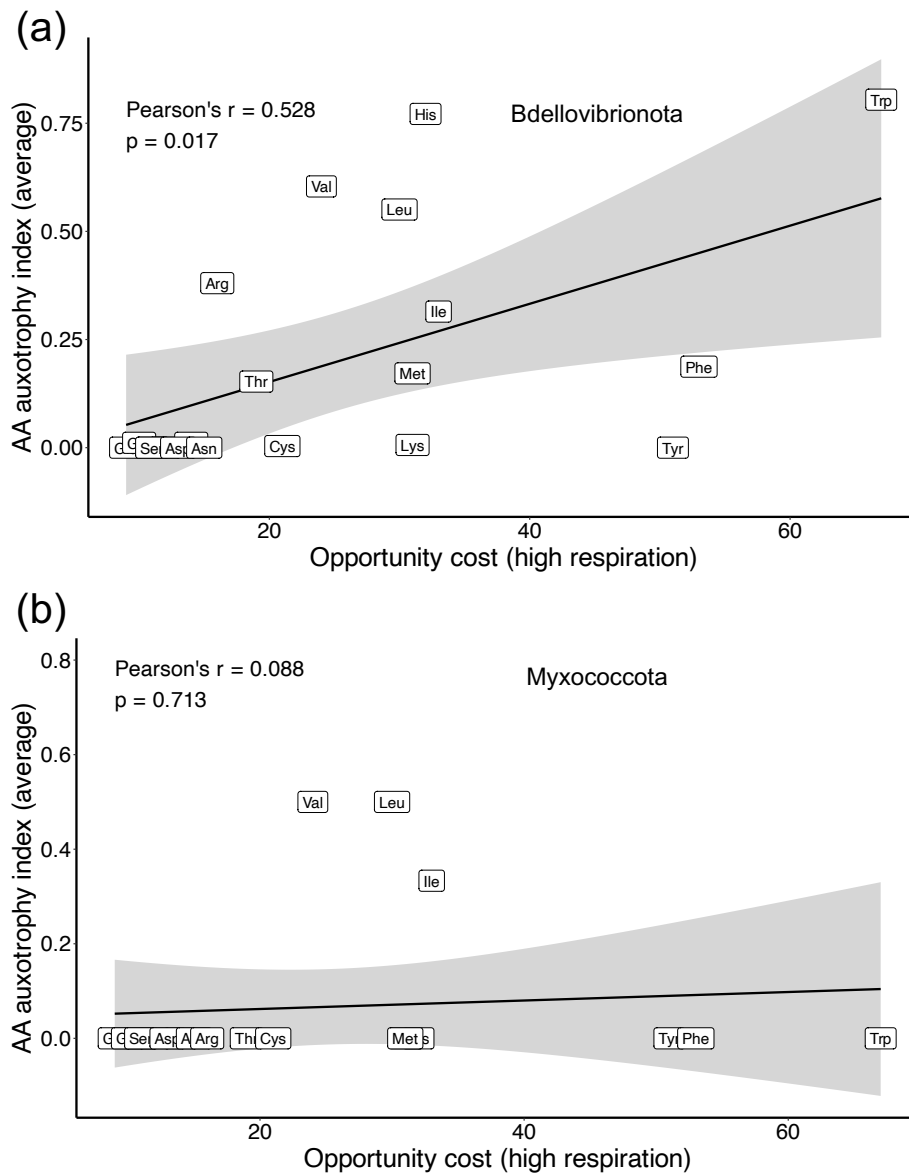


116

117 **Figure 1.** Completeness score of AA biosynthesis pathways in Bdellovibrionota and
118 Myxococcota. We created a database of 89 Bdellovibrionota and 203 Myxococcota proteomes
119 to get a comprehensive overview of AA dispensability in these groups. Full figure is shown in
120 File S1. We retrieved all enzymes involved in AA biosynthesis from the KEGG and MetaCyc
121 databases (reference collection) and searched for their homologs within our

122 Bdellovibrionota/Myxococcota database using MMseqs2 (see Methods). For each AA, we
123 showed a completeness score, which represents the percentage of enzymes within a pathway
124 that returned significant sequence similarity matches to our reference collection of AA
125 biosynthesis enzymes. In the case of AAs with multiple alternative pathways, we showed the
126 results only for the most complete one.

127 To globally test whether energy-related selection influences the observed reductions in AA
128 biosynthesis pathways of Bdellovibrionota and Myxococcota, we correlated the average AA
129 auxotrophy index with opportunity costs calculated under high respiration mode [5], a metric
130 that estimates the impact of AA biosynthesis on the cell's energy budget. To obtain the average
131 AA auxotrophy index for a given AA, we first subtracted the completeness score from 1
132 (Material and Methods, Equation 1) and then averaged the resulting AI values across all
133 considered proteomes. We detected a significant correlation between higher biosynthesis costs
134 and the loss of AA biosynthetic ability in Bdellovibrionota (Figure 2A). This suggests that
135 selection driven by energy management shaped the global pattern of auxotrophies in
136 Bdellovibrionota. As might be expected considering heatmap pattern (Figure 1), this broad-
137 scale analysis did not detect a positive correlation in Myxococcota, which are prototrophic for
138 most AAs (Figure 2B).



139

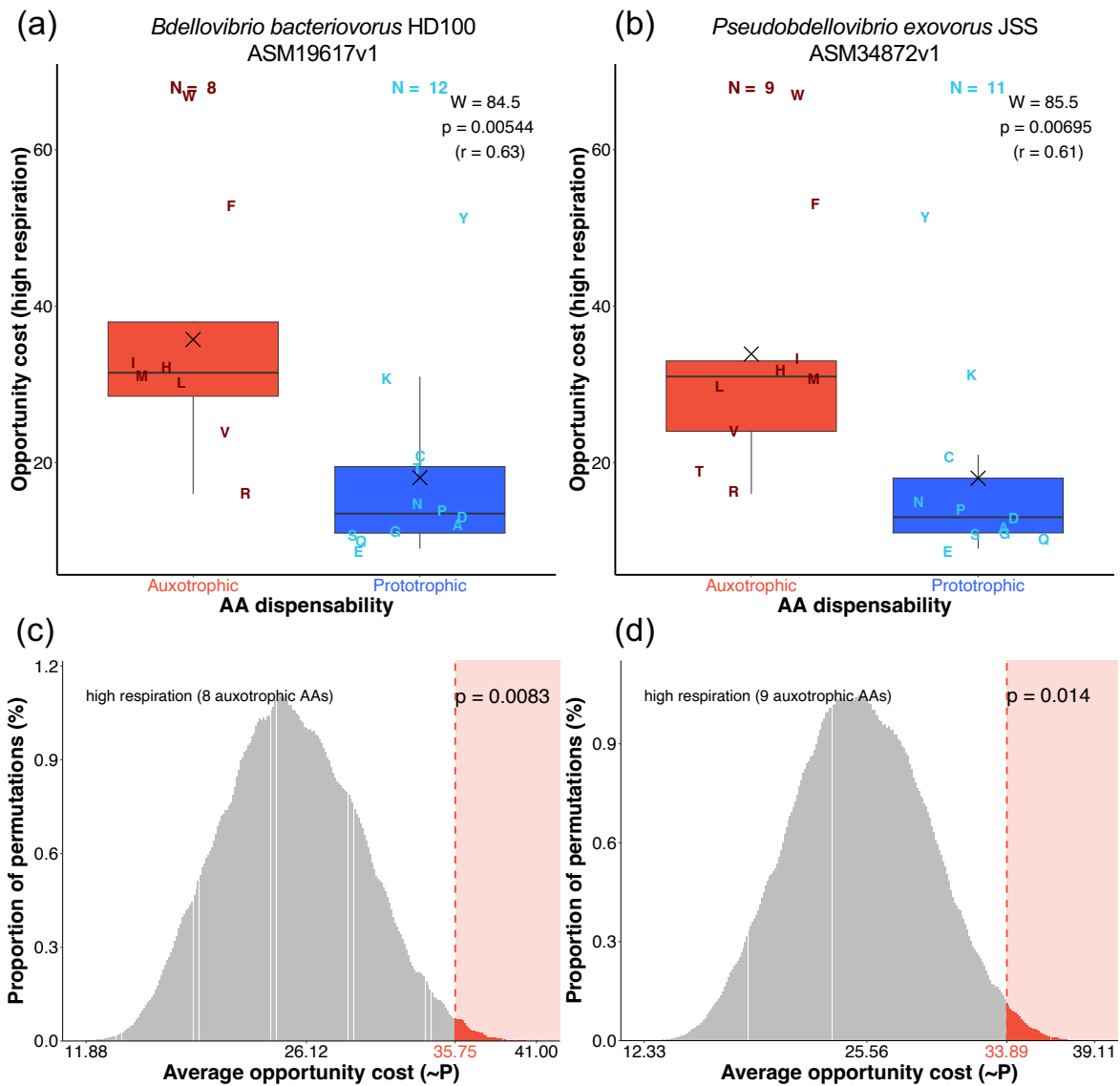
140 **Figure 2.** Correlation between AA biosynthesis cost and the average AA auxotrophy index. We
141 estimated the AA auxotrophy index (AI), a measure which equals one minus completeness
142 score (see Materials and Methods, Equation 1), for 89 Bdellovibrionota (a) and 203
143 Myxococcota (b) proteomes and calculated the average value for every AA. We correlated this
144 value with the opportunity cost of each AA, calculated for high respiration mode (see Materials
145 and Methods). Pearson correlation coefficient and p-value are shown on the graph.

146 To further evaluate whether the observed reductions in AA biosynthesis pathways in
147 Bdellovibrionota and Myxococcota result from energy-optimizing selection, we analyzed AA
148 auxotrophy patterns at the species level. To achieve this, we first explicitly determined the AA
149 auxotrophy status of each species by transforming the completeness score to binary values
150 (auxotrophic/prototrophic) (see Materials and Methods, Table S2). Although this procedure

151 reduces the information contained in the completeness scores, it allowed us to test the impact
152 of energy-related selection more directly by explicitly defining auxotrophic and prototrophic
153 AAs. In principle, the loss of even a single enzyme within a biochemical pathway could render
154 that pathway nonfunctional. Thus, we assigned auxotrophy status to any AA whose biosynthesis
155 pathway was incomplete. Using this binary-transformed dataset, we statistically compared
156 opportunity costs between auxotrophic and prototrophic AAs within each species [1]. In
157 addition, we applied a permutation-based selection test to assess the probability that the
158 observed constellation of auxotrophic AAs evolved under energy-related selection [1].

159 On average, Bdellovibrionota species exhibited 7.89 auxotrophic AAs per species (Table S2).
160 The comparison between auxotrophic and prototrophic AA sets using the Mann-Whitney non-
161 parametric test shows that auxotrophic AAs have significantly higher opportunity costs in 92%
162 of the 89 tested Bdellovibrionota species (Table S2; File S2). For illustration, we singled out
163 the results of this comparison for the type strains of *Bdellovibrio bacteriovorus* and
164 *Pseudobdellovibrio exovorius*, representing endobiotic and epibiotic lifestyles, respectively
165 (Figure 3). It is evident that, regardless of feeding ecology, auxotrophic AAs are significantly
166 more expensive than prototrophic ones (Figure 3A,B). The permutation-based selection test
167 revealed similar global trends, detecting that energy-related selection impacted the observed
168 distribution of auxotrophic AAs in 61% of Bdellovibrionota species (Table S2; File S2). For
169 instance, the average opportunity cost of the auxotrophic AA sets observed in *Bdellovibrio*
170 *bacteriovorus* and *Pseudobdellovibrio exovorius* falls at the right end of the distribution of all
171 possible permutations (Figure 3C,D). This indicates, just like in animals, that energy-optimizing
172 selection governed the outsourcing of auxotrophic AAs in these bacteria.

173 The trends are quite different in Myxococcota, where an average of 2.79 AAs are auxotrophic
174 (Table S2). The Mann-Whitney non-parametric test shows that auxotrophic AAs have
175 significantly higher opportunity costs in only 9% of the 203 tested species (Table S2; File S2).
176 In comparison, the permutation-based selection test revealed similar results, indicating that
177 energy-related selection impacted AA auxotrophies in only 7% of Myxococcota species (Table
178 S2). A prominent representative of Myxococcota that shows the impact of energy-related
179 selection on AA auxotrophies is *Pajaroellobacter abortibovis*, a species whose pathogenic
180 ecology differs from the facultative predatory lifestyle of most other Myxococcota (File S1,
181 Table S2, File S2). Taken together, these findings suggest that energy-optimizing selection
182 related to AA auxotrophies is rather rare among Myxococcota compared to Bdellovibrionota.

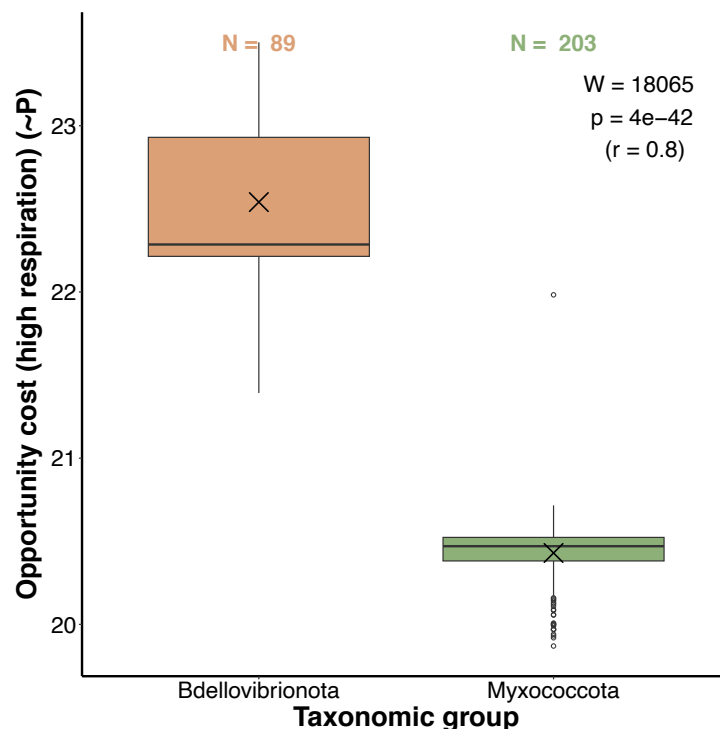


183

184 **Figure 3.** Comparisons of auxotrophic and prototrophic AA sets in *Bdellovibrio bacteriovorus*
 185 (A, C) and *Pseudobdellovibrio exovorius* (B, D). (A, B) The comparison of opportunity costs in
 186 high respiration mode between auxotrophic and prototrophic AA groups was tested by the
 187 Mann-Whitney U test with continuity correction. The corresponding W-value, p-value, and
 188 effect size (r) are depicted in each panel. The X symbol represents the mean. Individual AAs
 189 are shown by one-letter symbols. (C, D) Permutation analyses of opportunity costs (selection
 190 tests) were performed by calculating the average opportunity cost of every possible permutation
 191 for the number of auxotrophic AAs identified in a given species (n = 8 *B. bacteriovorus*, n = 9
 192 *P. exovorius*). The proportions of these averages are shown in histograms. The obtained
 193 distribution represents the empirical probability mass function (PMF). The value in red denotes
 194 the average opportunity cost value of the EAA sets observed in nature. The p-value was
 195 calculated by summing the proportions that correspond to average opportunity cost values equal

196 to, or more extreme, than the observed value. Low p-values indicate a high probability that
197 energy-related selection drove the loss of auxotrophic AA biosynthesis capability.

198 The fact that Bdellovibrionota converge to an animal-like set of amino acid (AA) auxotrophies,
199 while closely related Myxococcota remain mainly prototrophic, allows us to further test the
200 predictions of our model [1]. In our previous work, we showed that animals code for
201 significantly more expensive proteomes, compared to Choanoflagellates, their sister group
202 which is mainly prototrophic [1]. We proposed that animals have more expensive proteomes
203 than Choanoflagellates, likely because they consume less energy on AA biosynthesis and are
204 thus able to maintain a larger number of expensive auxotrophic AAs in their proteomes [1].
205 Using a non-parametric test to compare the opportunity costs (high respiration mode) of an
206 average AA in bacterial proteomes (Material and Methods, Equation 2), we recovered an
207 analogous result: the proteomes of the more auxotrophic Bdellovibrionota are significantly
208 more expensive than those of the more prototrophic Myxococcota (Figure 4), underscoring the
209 universality of energy-related selection on proteome composition.



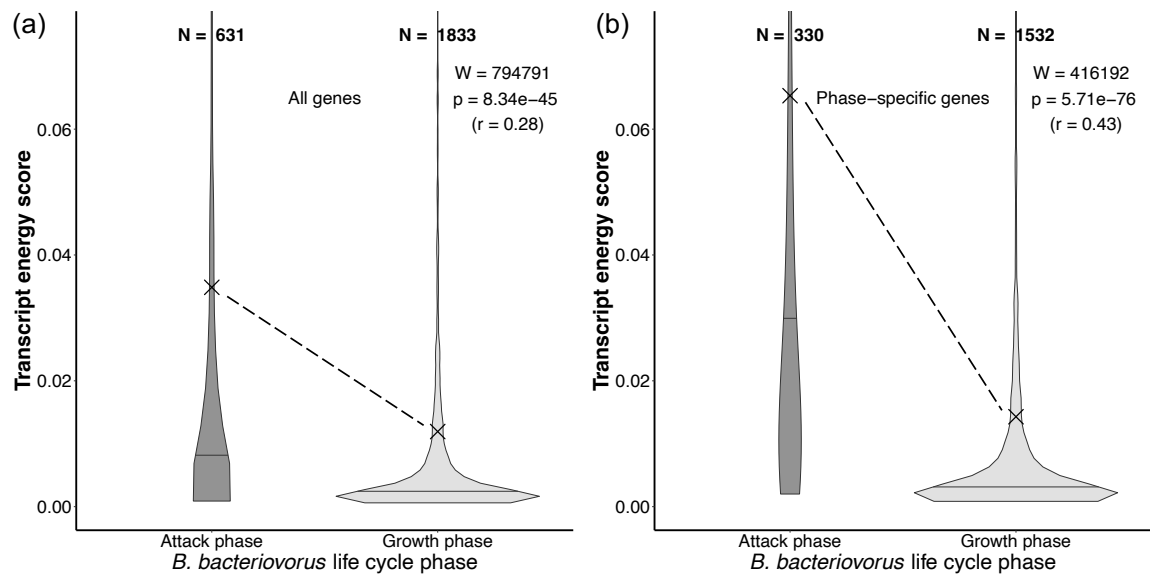
210

211 **Figure 4.** The comparison of the opportunity cost (OC) of an average AA in proteomes of
212 Bdellovibrionota and Myxococcota. The opportunity cost under high respiration mode (OC) of
213 an average AA in a proteome represents a weighted mean of AA biosynthesis energy costs
214 where the frequencies of twenty AAs in the proteome act as weights. The differences in energy
215 costs between the two groups were shown by boxplots and the significance of these differences

216 was tested by the Mann-Whitney U test with continuity correction. We depicted the
217 corresponding W-value, p-value, and effect size (r) in each panel. The X symbol represents the
218 mean. The list of Bdellovibrionota (89) and Myxococcota (203) whose proteomes are included
219 in calculations is available in Supplementary Data X.

220 Finally, we used the published transcriptome data to examine the energetics of the two
221 distinct phases in the life cycle of *Bdellovibrio bacteriovorus*: the attack phase and the growth
222 phase [14]. For each transcript, we calculated its frequency in the transcriptome at a given life
223 cycle phase [22]. We then multiplied this transcript frequency by the opportunity cost of an
224 average amino acid (AA) encoded by that transcript (OC_{protein}) (Equations 3 and 4). This
225 measure, which we named the transcript energy score (TES), couples transcript levels in the
226 cell with the encoded protein costs (see Material and Methods). Higher TES values reflect
227 greater impact, while lower TES values indicate a smaller impact of a given transcript on the
228 total energy budget of the cell. We performed the TES-based analysis in two ways: by including
229 all genes expressed per phase and by considering only those which were exclusively expressed
230 in one phase (Figure 5).

231 The attack phase is generally characterized by a much smaller number of expressed genes,
232 which are more evenly distributed across the narrower range of TES values (Figure 5). In
233 contrast, the TES values of the growth phase are predominantly grouped at the lower end of the
234 TES range. This suggests that the attack phase of predatory *B. bacteriovorus* is underpinned by
235 high transcription of a relatively small number of genes many of which encode expensive
236 proteins. In contrast, the growth phase is characterized by relatively low transcription of many
237 genes that encode cheaper proteins. These differences are even more apparent in the analysis of
238 phase-specific genes (Figure 5B). Together, this suggests that the active predation in *B.*
239 *bacteriovorus* requires proteins which are composed of expensive AAs. As an analogy, we
240 previously speculated that similar phenotypes might exist in the context of animal predation
241 [1].



242

243 **Figure 5.** The comparison of transcriptome energy scores (TES) between two phases in the life
 244 cycles of *B. bacteriovorus*. Calculations were performed (a) for all genes that are expressed per
 245 phase and (b) only for phase-specific genes. The TES value represents the average opportunity
 246 cost of a gene product multiplied by its frequency in the transcriptome at a given life cycle
 247 phase. The significance of the difference between the two phases was tested by the Mann-
 248 Whitney U test with continuity correction. We depicted the corresponding W-value, p-value,
 249 and effect size (r). Outliers were removed from the graph for the clarity of presentation, but
 250 were included in the calculation of statistics. The X symbol represents the mean, and the
 251 horizontal line within a violin-plot represents the median. Transcription data was retrieved from
 252 Karunker et al. 2013 (Karunker et al., 2013).

253

254 Discussion

255 Functional outsourcing presumes that genes that support essential functions can be lost from
 256 the genome if their activity can be substituted through environmental interactions [8]. We have
 257 successfully applied this concept to the evolution of AA auxotrophies in animals and bacteria
 258 [1,5]. We found that all animals and some bacterial groups which are capable of harvesting a
 259 sufficient amount of AAs from their ecosystem lose the ability to produce expensive AAs on
 260 their own [1,5,8]. This AA outsourcing is at least partially driven by energy-optimizing
 261 selection, which not only favors the loss of the ability to synthesize expensive AAs but also
 262 allows for more frequent usage of expensive AAs in the proteome [1,5]. We proposed that these
 263 phenotypes could have been triggered in animals by predation and aerobic respiration [1]. If

264 these processes are indeed selection-driven, it would be expected that they occur convergently
265 under similar ecological pressures across the tree of life.

266 Unlike most other bacteria, Bdellovibrionota and Myxococcota are aerobic predators; they hunt
267 and consume their bacterial prey under aerobic or microaerobic conditions [11–13,23]. As an
268 independent evolutionary event, these behaviors were likely crucial for the outsourcing of AA
269 production in animals [1]. We have shown here that obligate aerobic predation left an
270 astonishingly similar metabolic impact on Bdellovibrionota, resulting in the largely overlapping
271 set of AA auxotrophies compared to animals. In contrast, very few auxotrophies can be
272 observed in Myxococcota, which are facultative predators [18,20].

273 There are likely multiple factors that influenced the vast differences in AA biosynthesis
274 capabilities between Bdellovibrionota and Myxococcota. However, the most apparent and
275 potentially vital factor is that Myxococcota are only facultatively predatory [18], making them
276 unable to consistently obtain AAs in large quantities. This is supported by the observation that
277 Bdellovibrionota grow and assimilate carbon at higher rates than Myxococcota [18].
278 Furthermore, it has been observed that Bdellovibrionota are significantly more abundant in
279 aerobic environments than in anaerobic ones, in contrast to Myxococcota, which show no
280 apparent preference [23]. This might indicate that the metabolism of Bdellovibrionota is more
281 dependent on efficient respiration, which could also drive them toward heightened AA
282 auxotrophy levels [1]. Another important factor might be feeding efficiency—Bdellovibrionota
283 are always physically connected to their prey, while Myxococcota secrete hydrolytic enzymes
284 around their prey, which carries the risk of diffusion, leading to a lower return of the energy
285 expended on predation [24].

286 The reduction in the ability to synthesize expensive AAs is directly correlated with the increased
287 usage of expensive AAs in the proteomes [1,5]. Animals use more frequently expensive AAs
288 in their proteomes than their sister group, choanoflagellates, and here we showed that the same
289 is true for Bdellovibrionota when compared to their related group, Myxococcota [15]. Although
290 Myxococcota have larger proteomes than Bdellovibrionota [11,24], their encoded AAs are on
291 average cheaper by a large margin, which suggests that their complex lifestyle requires a wide
292 range of functions that do not require proteins with very expensive AAs.

293 On the other hand, the ecology of Bdellovibrionota is relatively simple, consisting of two
294 distinct phases: the attack phase, during which cells actively hunt, and the growth phase, during
295 which cells consume their prey and subsequently divide [11,12,14]. A previous study produced

296 transcriptome data for these two phases in *B. bacteriovorus* [14], providing a unique
297 opportunity to examine the effects of energy-related selection on the *B. bacteriovorus* life cycle.
298 We used a novel measure, the transcript energy score (TES), which combines the energy cost
299 of a coding gene with its level of transcription, producing higher scores for more expensive and
300 highly expressed transcripts. Using this metric, we found that the growth phase is underlined
301 by a much larger set of transcripts with relatively similar expression levels that encode for
302 cheaper AAs, while the attack phase consists of a relatively small subset of transcripts with a
303 wide range of expression levels that encode for more expensive AAs. This supports the
304 possibility that the energy saved through the outsourcing of AAs was invested in the attack
305 phase, enabling more efficient predatory behavior and thus ensuring a more consistent influx
306 of AAs from the environment, creating a positive feedback loop.

307 In conclusion, it is evident that every level of biological organization—from metabolism and
308 proteome composition to the regulation of gene transcription—is intimately tied to the
309 organism's energy budget. The repeated convergent evolution of similar sets of AA
310 auxotrophies across eukaryotes and prokaryotes can be attributed to obligate predation under
311 aerobic conditions, which itself goes hand in hand with the evolution of novel and expensive
312 predation-related functions. Deeper understanding of the evolutionary pressures leading to
313 predatory behavior in bacteria is especially important, as it has implications not only for
314 understanding the regulation of ecological networks [18] but also for potential medical
315 applications [25].

316

317 **Materials and Methods**

318 All proteomes used in this study were retrieved from the NCBI GenBank. We acquired the
319 highest-quality Bdellovibrionota (89) and Myxococcota (203) proteomes by using the NCBI
320 filter to exclude atypical genomes, metagenome-assembled genomes, and genomes from large
321 multi-isolate projects.

322

323 We conducted the detection of amino acid (AA) biosynthesis pathway completeness using the
324 protocol described in our earlier publication [5]. Briefly, we prepared a reference database of
325 387,892 enzyme sequences across 2,095 bacterial species, with each enzyme annotated with
326 the biosynthetic pathway it is involved in [5]. We combined the reference database with our

327 proteomes and clustered the sequences using MMseqs2 [21] with the following parameters: -
328 cluster-mode 0, -cov-mode 0, -c 0.8, and -e 0.001. We then functionally annotated all members
329 of a cluster based on the presence of enzymes from the reference database in that cluster.

330 For each AA biosynthesis pathway and species in the database, we calculated a pathway
331 completeness score (i.e., prototrophy index) by dividing the number of detected enzymes by
332 the total number of enzymes in that pathway,s resulting in values ranging from 0 to 1. If a
333 species contained alternative biosynthetic pathways for an AA, the pathway with the highest
334 completeness score was selected. We then calculated the AA auxotrophy index of the i-th amino
335 acid (AI_i) by subtracting the completeness score from 1 [5]:

$$336 \quad AI_i = 1 - \text{completness score} \quad (1)$$

337 We used the energy costs of AA biosynthesis as described in our earlier publications [1,5]. The
338 opportunity cost reflects the impact of AA synthesis on the cell's energy budget and is calculated
339 as the sum of the energy lost in the synthesis of AAs (direct cost) and the energy that would
340 have been produced if a cell catabolized precursors instead of making AAs. Using the AA
341 opportunity cost, we also calculated the opportunity cost of an average AA in each proteome
342 ($OC_{proteome}$) using the following equation:

$$343 \quad OC_{proteome} = \frac{\sum_{i=1}^{n=20} OC_i \times N_i}{\sum_{i=1}^{n=20} N_i} = \sum_{i=1}^{n=20} OC_i \times F_i \quad (2)$$

344 In this equation, OC_i represents the opportunity cost of the i-th AA, N_i denotes the total number
345 of occurrences of this AA in the entire proteome, and F_i represents the frequency of the AA in
346 the proteome.

347 The permutation analyses were performed separately for each species by first determining the
348 number of auxotrophic AAs and then generating all possible permutations for that number of
349 auxotrophic AAs. For each permutation, we then calculated the average opportunity cost of the
350 auxotrophic AAs. For example, if a species was found to be auxotrophic for 10 AAs, we found
351 all possible combinations of 10 AAs and calculated the average opportunity cost of each. Since
352 there is a limited number of possible average values, each value was treated as a bin. We
353 calculated the proportion of permutations within a bin by dividing the number of elements in
354 that bin by the total number of permutations. The obtained distribution represents empirical
355 probability mass function (PMF) which was then used to calculate the probability that the
356 observed set of auxotrophies in a given species is a result of a random process. We calculated

357 p-values by summing the proportions of permutation in the range from the actual value observed
358 in nature to the most extreme value at the closest distribution tail [1].

359 For transcriptome analysis, we obtained data on differential gene expression in the two distinct
360 life cycle phases of *Bdellovibrio bacteriovorus* from an earlier study [14]. For each gene (i), we
361 calculated its proportion in a given transcriptome phase by dividing its transcription value (t_i)
362 by the sum of all transcription values in that phase. This proportion in essence represents the
363 frequency of each transcript in the transcriptome phase ($f_{transcript}$). We then multiplied this
364 number by the opportunity cost (high respiration mode) of the protein encoded by that gene
365 ($OC_{protein}$) to obtain a transcript energy score (TES). This score is meant to represent the energy
366 impact of each transcript on the total energy budget of a transcriptome phase. TES was
367 calculated using the following equation:

$$368 \quad TES_i = \frac{t_i}{\sum_i t_i} \times OC_{protein} = f_{transcript} \times OC_{protein} \quad (3)$$

369 The opportunity cost of proteins was calculated using the following equation:

$$370 \quad OC_{protein} = \frac{\sum_{i=1}^{n=20} OC_i \times n_i}{\sum_{i=1}^{n=20} n_i} = \sum_{i=1}^{n=20} OC_i \times f_i \quad (4)$$

371 In this equation, OC_i represents the opportunity cost of the i-th AA, n_i denotes the total number
372 of occurrences of this AA in the protein, and f_i represents the frequency of the AA in the protein.

373 We used the Mann-Whitney U test with continuity correction to compare the opportunity costs
374 of an average AA in proteomes ($OC_{proteome}$) of Bdellovibrionota and Myxococcota using the
375 package rcompanion (<https://CRAN.R-project.org/package=rcompanion>). We used the same
376 test to compare transcript energy scores (TES) of different life cycle phases in *B. bacteriovorus*.
377 To calculate correlations, we used the `cor.test()` function in the R stats (v. 3.6.2) package. The
378 heatmap was visualized using the ComplexHeatmap package [26].

379 **Supplementary Materials:** File S1: Full pathway completeness heatmap; File S2: Per-species
380 statistics on binary encoded auxotrophies; Table S1: Database with pathway completeness
381 detection results.xlsx; Table S2: Summary of statistics based on binary encoding of
382 auxotrophies

383 **Author Contributions:** Conceptualization, N.K., M.D.-L. and T.D.-L.; methodology, N.K.,
384 M.D.-L. and T.D.-L.; software, N.K. and M.D.-L.; validation, N.K., M.D.-L. and T.D.-L.;
385 formal analysis, N.K., M.D.-L. and T.D.-L.; writing—original draft preparation, N.K., M.D.-L.

386 and T.D.-L.; writing—review and editing, N.K., M.D.-L. and T.D.-L.; visualization, N.K. and
387 M.D.-L.; supervision, M.D.-L. and T.D.-L. All authors have read and agreed to the published
388 version of the manuscript.

389 **Funding:** This work was supported by the European Regional Development Fund
390 KK.01.1.1.01.0009 DATACROSS (M.D.-L., T.D.-L.).

391 **Data Availability Statement:** All data are available in the supplementary materials.

392 **Acknowledgments:** We thank M. Futo, A. Tušar, S. Koska, D. Franjević and G. Klobučar for
393 discussions. We used the computational resources of the University Computing Center - SRCE
394 (Padobran) and the Institute Ruđer Bošković.

395 **Conflicts of Interest:** The authors declare no conflicts of interest.

396

397 **References**

398 1. Kasalo, N.; Domazet-Lošo, M.; Domazet-Lošo, T. Massive Outsourcing of Energetically
399 Costly Amino Acids at the Origin of Animals. *bioRxiv* 2024,
400 <https://doi.org/10.1101/2024.04.18.590100>.

401 2. Payne, S.H.; Loomis, W.F. Retention and Loss of Amino Acid Biosynthetic Pathways
402 Based on Analysis of Whole-Genome Sequences. *Eukaryot. Cell* 2006, *5*, 272–276,
403 doi:10.1128/ec.5.2.272-276.2006.

404 3. Trolle, J.; McBee, R.M.; Kaufman, A.; Pinglay, S.; Berger, H.; German, S.; Liu, L.; Shen,
405 M.J.; Guo, X.; Martin, J.A.; et al. Resurrecting Essential Amino Acid Biosynthesis in
406 Mammalian Cells. *eLife* 2022, *11*, e72847, doi:10.7554/eLife.72847.

407 4. Ramoneda, J.; Jensen, T.B.N.; Price, M.N.; Casamayor, E.O.; Fierer, N. Taxonomic and
408 Environmental Distribution of Bacterial Amino Acid Auxotrophies. *Nat. Commun.* 2023, *14*,
409 7608, doi:10.1038/s41467-023-43435-4.

410 5. Kasalo, N.; Domazet-Lošo, T.; Domazet-Lošo, M. Bacterial Amino Acid Auxotrophies
411 Enable Energetically Costlier Proteomes. *bioRxiv* 2025,
412 <https://doi.org/10.1101/2025.01.24.634666>.

413 6. Starke, S.; Harris, D.M.M.; Zimmermann, J.; Schuchardt, S.; Oumari, M.; Frank, D.; Bang,
414 C.; Rosenstiel, P.; Schreiber, S.; Frey, N.; et al. Amino Acid Auxotrophies in Human Gut

- 415 Bacteria Are Linked to Higher Microbiome Diversity and Long-Term Stability. *ISME J.* 2023,
416 17, 2370–2380, doi:10.1038/s41396-023-01537-3.
- 417 7. D’Souza, G.; Waschina, S.; Pande, S.; Bohl, K.; Kaleta, C.; Kost, C. Less Is More:
418 Selective Advantages CAN Explain the Prevalent Loss of Biosynthetic Genes in Bacteria.
419 *Evolution* 2014, 68, 2559–2570, doi:10.1111/evo.12468.
- 420 8. Domazet-Lošo, M.; Široki, T.; Šimičević, K.; Domazet-Lošo, T. Macroevolutionary
421 Dynamics of Gene Family Gain and Loss along Multicellular Eukaryotic Lineages. *Nat.*
422 *Commun.* 2024, 15, 2663, doi:10.1038/s41467-024-47017-w.
- 423 9. Lozupone, C.A.; Knight, R. Global Patterns in Bacterial Diversity. *Proc. Natl. Acad. Sci.*
424 2007, 104, 11436–11440, doi:10.1073/pnas.0611525104.
- 425 10. Price, M.N.; Zane, G.M.; Kuehl, J.V.; Melnyk, R.A.; Wall, J.D.; Deutschbauer, A.M.;
426 Arkin, A.P. Filling Gaps in Bacterial Amino Acid Biosynthesis Pathways with High-
427 Throughput Genetics. *PLOS Genet.* 2018, 14, e1007147, doi:10.1371/journal.pgen.1007147.
- 428 11. Sockett, R.E. Predatory Lifestyle of *Bdellovibrio Bacteriovorus*. *Annu. Rev. Microbiol.*
429 2009, 63, 523–539, doi:10.1146/annurev.micro.091208.073346.
- 430 12. Wang, Z.; Kadouri, D.E.; Wu, M. Genomic Insights into an Obligate Epibiotic Bacterial
431 Predator: *Micavibrio Aeruginosavorus* ARL-13. *BMC Genomics* 2011, 12, 453,
432 doi:10.1186/1471-2164-12-453.
- 433 13. Ye, X.-S.; Chen, M.-X.; Li, H.-Y.; He, X.-Y.; Zhao, Y. Halobacteriovorax *Vibrionivorans*
434 Sp. Nov., a Novel Prokaryotic Predator Isolated from Coastal Seawater of China. *Int. J. Syst.*
435 *Evol. Microbiol.* 2019, 69, 3917–3923, doi:10.1099/ijsem.0.003703.
- 436 14. Karunker, I.; Rotem, O.; Dori-Bachash, M.; Jurkevitch, E.; Sorek, R. A Global
437 Transcriptional Switch between the Attack and Growth Forms of *Bdellovibrio Bacteriovorus*.
438 *PLoS ONE* 2013, 8, e61850, doi:10.1371/journal.pone.0061850.
- 439 15. Davis, S.C.; Cerra, J.; Williams, L.E. Comparative Genomics of Obligate Predatory
440 Bacteria Belonging to Phylum *Bdellovibrionota* Highlights Distribution and Predicted
441 Functions of Lineage-Specific Protein Families. *mSphere* 2024, 9, e00680-24,
442 doi:10.1128/msphere.00680-24.
- 443 16. Waite, D.W.; Chuvochina, M.; Pelikan, C.; Parks, D.H.; Yilmaz, P.; Wagner, M.; Loy, A.;
444 Naganuma, T.; Nakai, R.; Whitman, W.B.; et al. Proposal to Reclassify the Proteobacterial

445 Classes Deltaproteobacteria and Oligoflexia, and the Phylum Thermodesulfobacteria into
446 Four Phyla Reflecting Major Functional Capabilities. *Int. J. Syst. Evol. Microbiol.* 2020, 70,
447 5972–6016, doi:10.1099/ijsem.0.004213.

448 17. Cao, P.; Dey, A.; Vassallo, C.N.; Wall, D. How Myxobacteria Cooperate. *J. Mol. Biol.*
449 2015, 427, 3709–3721, doi:10.1016/j.jmb.2015.07.022.

450 18. Hungate, B.A.; Marks, J.C.; Power, M.E.; Schwartz, E.; Van Groenigen, K.J.; Blazewicz,
451 S.J.; Chuckran, P.; Dijkstra, P.; Finley, B.K.; Firestone, M.K.; et al. The Functional
452 Significance of Bacterial Predators. *mBio* 2021, 12, e00466-21, doi:10.1128/mBio.00466-21.

453 19. Kaiser, D.; Robinson, M.; Kroos, L. Myxobacteria, Polarity, and Multicellular
454 Morphogenesis. *Cold Spring Harb. Perspect. Biol.* 2010, 2, a000380–a000380,
455 doi:10.1101/cshperspect.a000380.

456 20. Reichenbach, H. The Ecology of the Myxobacteria. *Environ. Microbiol.* 1999, 1, 15–21,
457 doi:10.1046/j.1462-2920.1999.00016.x.

458 21. Steinegger, M.; Söding, J. MMseqs2 Enables Sensitive Protein Sequence Searching for
459 the Analysis of Massive Data Sets. *Nat. Biotechnol.* 2017, 35, 1026–1028,
460 doi:10.1038/nbt.3988.

461 22. Domazet-Lošo, T.; Tautz, D. A Phylogenetically Based Transcriptome Age Index Mirrors
462 Ontogenetic Divergence Patterns. *Nature* 2010, 468, 815–818, doi:10.1038/nature09632.

463 23. Zhang, L.; Huang, X.; Zhou, J.; Ju, F. Active Predation, Phylogenetic Diversity, and
464 Global Prevalence of Myxobacteria in Wastewater Treatment Plants. *ISME J.* 2023, 17, 671–
465 681, doi:10.1038/s41396-023-01378-0.

466 24. Muñoz-Dorado, J.; Marcos-Torres, F.J.; García-Bravo, E.; Moraleda-Muñoz, A.; Pérez, J.
467 Myxobacteria: Moving, Killing, Feeding, and Surviving Together. *Front. Microbiol.* 2016, 7,
468 doi:10.3389/fmicb.2016.00781.

469 25. Sockett, R.E.; Lambert, C. Bdellovibrio as Therapeutic Agents: A Predatory Renaissance?
470 *Nat. Rev. Microbiol.* 2004, 2, 669–675, doi:10.1038/nrmicro959.

471 26. Gu, Z. Complex Heatmap Visualization. *iMeta* 2022, 1, e43, doi:10.1002/imt2.43.

472